Vol 14 No 1, January 2005
1009-1963/2005/14(01)/0163-06

Chinese Physics

© 2005 Chin. Phys. Soc.
and IOP Publishing Ltd

Two-dimensional temperature distribution inside a hemispherical bowl-shaped target for plasma source ion implantation*

Liu Cheng-Sen(刘成森)[a)b)], Wang Yan-Hui(王艳辉)[a)], and Wang De-Zhen(王德真)[a)†]

[a)] *State Key Laboratory for Materials Modification by Laser, Ion and Electron Beams, Department of Physics, Dalian University of Technology, Dalian* 116023, *China*

[b)] *Department of Physics, Liaoning Normal University, Dalian* 116029, *China*

(Received 1 April 2004; revised manuscript received 14 August 2004)

One important parameter for the plasma source ion implantation (PSII) process is the target temperature obtained during the surface modification. Because the power input to the target being implanted can be large, its temperature is quite high. The target temperature prediction is useful, whether the high temperature is required in the experiment. In addition, there is likely to be temperature variation across the target surface, which can lead to locally different surface properties. In this paper, we have presented a model to predict and explain the temperature distribution on a hemispherical bowl-shaped vessel during plasma source ion implantation. A two-dimensional fluid model to derive both the ion flux to the target and the energy imparted to the substrate by the ions in the plasma sheath simulation is employed. The calculated energy input and radiative heat loss are used to predict the temperature rise and variation inside the sample in the thermal model. The shape factor of the target for radiation is taken into account in the radiative energy loss. The influence of the pulse duration and the pulsing frequency on the temperature distribution is investigated in detail. Our work shows that at high pulsing frequencies the temperature of the bowl will no longer rise with the increase of the pulsing frequency.

Keywords: hemispherical bowl-shaped vessel, plasma source ion implantation, ion heating
PACC: 5225L, 5250G, 5250K

1. Introduction

Plasma source ion implantation (PSII)[1] is a versatile method for surface modification, and many efforts have been made to use this method in various practical applications. Because there is no line-of-sight restriction, it is an excellent technique to treat industrial work pieces with irregular shapes. PSII has been used to improve the wear, corrosion, and fatigue resistance of metals and in the fabrication of semiconductors.[2−4] PSII is also used to create a graded interface on the surface to enhance the adhesion of subsequently deposited coatings.[5,6] PSII incorporates the strong points of other plasma treatments, like plasma nitriding and ion implantation.

In the PSII process, when negative voltage pulses are applied to the target, the ion bombardment serves as a heating process and induces a high target temperature. The temperature obtained during the process is crucial to the final surface properties. High temperature is desirable, for instance, when diffusion of the implanted ion is desirable. In the case of stainless steel, its treated temperature exceeding 450°C can lead to CrN precipitation, whereas at a temperature below 350°C, nitrogen diffusion is too slow to result in a sufficiently thick layer suitable for application.[7−9] Meanwhile an elevated temperature process increases substantially the wear-resistance without sacrifice of the corrosion-resistance. A direct measurement of the target temperature is highly desirable in PSII, but in practice it is not as easy as one imagines, because the process environment (high voltage, vacuum, interface, etc) renders common techniques for measuring temperature impractical. Optical measurement is a realistic option for on-line temperature measurement, but it is not widely used because optical measurement of temperature can be expensive and it only yields

*Project supported by National Natural Science Foundation of China (Grant No 10275010).
†E-mail: wangdez@dlut.edu.cn

surface temperature. Therefore it is important to develop a model to map the temperature gradient over the target. Blanchard has developed a simple, time-dependent, lumped-capacity thermal model for predicting temperatures in PSII targets. Unfortunately, this model cannot provide multidimensional temperature information. Since the ion flux depends on the sample geometry, there are likely to be local temperature fluctuations that alter the local structure and properties. Recently a two-dimensional (2D) model for a round platen that takes into account the finite dimensions of the target has been described.[10] This model combines the plasma fluid model with the unsteady-state heat transfer equation. The ion flux is calculated by using the fluid model and input into the heat transfer equation to derive the temperature distribution on the target surface. This model can be conveniently applied to the metal or semiconductor PSII requiring strict temperature control. In this work, we describe our two-dimensional model to investigate the temperature distribution of a hemispherical bowl-shaped vessel in PSII process. In the model we take into account the influence of shape factor of the bowl on the radiation heat transfer from the target to the chamber.

2. Plasma sheath simulation and thermal model

Plasma ion bombardment during the PSII process is treated as a surface heat flux, because the ions actually deposit their energies on the target surface. To derive the target temperature, we use a 2D fluid model to calculate the incident ion flux by simulating the temporal sheath expansion.[11] Consider PSII into the surface of a hemispherical-bowl vessel, as shown in Fig.1. The inner radius of the vessel is $r_{\rm in}$ and the outer is $r_{\rm out}$. The vessel is immersed in a charge-neutral plasma in which the ion and electron densities $n_{\rm i}$ and $n_{\rm e}$ are both equal to the plasma density $n_{\rm o}$, i.e. $n_{\rm i} = n_{\rm e} = n_{\rm o}$. The initial potential is $\phi = 0$ everywhere. When the high negative voltage pulse is applied to the target, the electrons are repelled from the target. Ions are initially at rest, for the ion mass is much larger than the electron mass. Thus a plasma sheath is formed around the target. When $t > \omega_{\rm pi}^{-1}$ (where t is the duration for the pulse to be exerted on the target and $\omega_{\rm pi}$ is the ion plasma frequency), ions are accelerated by the electric field in the sheath and implanted into the target until the applied voltage pulse is over. The ion density, the ion velocity, and the potential then evolve self-consistently in time.

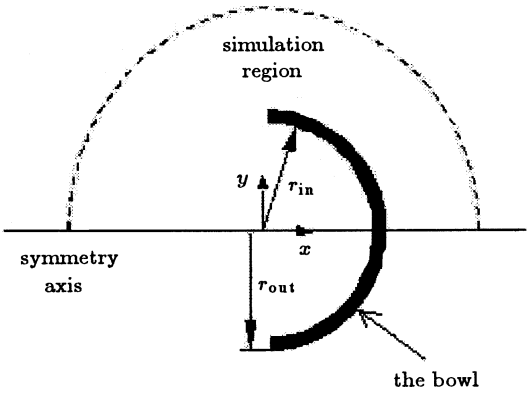


Fig.1. Schematic diagram of the implantation geometry considered.

The evolutions of the ion density, ion velocity, and potential are modelled using cold, collisionless fluid ions, Boltzmann electrons, and Poisson's equation. In spherical coordinates, the 2D equations of ion continuity and motion, and Poisson's equation respectively are

$$\frac{\partial n}{\partial \tau} + \frac{1}{R^2}\frac{\partial}{\partial R}(R^2 n u_R) + \frac{1}{R\sin\theta}\frac{\partial}{\partial \theta}(n u_\theta \sin\theta) = 0, \quad (1)$$

$$\frac{\partial u_R}{\partial \tau} + u_R\frac{\partial u_R}{\partial R} + \frac{u_\theta}{R}\frac{\partial u_R}{\partial \theta} = -\frac{\partial \varphi}{\partial R}, \quad (2)$$

$$\frac{\partial u_\theta}{\partial \tau} + u_R\frac{\partial u_\theta}{\partial R} + \frac{u_\theta}{R}\frac{\partial u_\theta}{\partial \theta} = -\frac{1}{R}\frac{\partial \varphi}{\partial \theta}, \quad (3)$$

$$\frac{\partial^2 \varphi}{\partial R^2} + \frac{1}{R}\frac{\partial \varphi}{\partial R} + \frac{\mathrm{ctg}\theta}{R^2}\frac{\partial \varphi}{\partial \theta} + \frac{1}{R^2}\frac{\partial^2 \varphi}{\partial \theta^2} = -[n - \exp(\varphi)]. \quad (4)$$

The normalized dimensionless variables are

$$\tau = t\omega_{\rm pi}, \quad R = r/\lambda_{\rm D}, \quad \varphi = e\phi/T_{\rm e},$$

$$n = n_{\rm i}/n_{\rm o}, \quad u_R = v_{\rm ir}/v_{\rm is}, \quad u_\theta = v_{\rm i\theta}/v_{\rm is}, \quad (5)$$

where $n_{\rm i}$ is the ion density, ϕ is the potential, e is the ionic charge (for a singly ionized ion), and m is the mass. $T_{\rm e}$ is the electron temperature, $\varepsilon_{\rm o}$ is the permittivity of free space, and $v_{\rm ir}$ and $v_{\rm i\theta}$ are the ion velocities in radial direction and in angular direction, respectively. $\lambda_{\rm D} = (\varepsilon_{\rm o}T_{\rm e}/n_{\rm o}e^2)^{1/2}$ is the Debye length, $v_{\rm is} = (T_{\rm e}/m)^{1/2}$ is the ion sound velocity, and $\omega_{\rm pi} = (n_{\rm o}e^2/m\varepsilon_{\rm o})^{1/2}$ is the ion plasma frequency. The normalized target potential is given by

$$\varphi = \begin{cases} \varphi_{\rm p}(\tau/\tau_{\rm r}), & \tau \le \tau_{\rm r}, \\ \varphi_{\rm p}, & \tau > \tau_{\rm r}, \end{cases} \quad (6)$$

where $\tau_{\rm r} = t_{\rm r}\omega_{\rm pi}$ is the dimensionless rise time, $\varphi_{\rm p} = e\phi_{\rm p}/T_{\rm e}$ is the dimensionless maximum potential biased on the target.

Equation (4) is solved by iteration. Setting ψ to be an initial guess for the solution, Eq.(4) is linearized about this guess using[12]

$$\exp(\varphi) = \exp(\psi)\exp(\varphi - \psi) \approx (1 + \varphi - \psi)\exp(\psi), \tag{7}$$

and after neglecting high-order terms, the linearized equation becomes

$$\frac{\partial^2\varphi}{\partial R^2} + \frac{1}{R}\frac{\partial\varphi}{\partial R} + \frac{\mathrm{ctg}\theta}{R^2}\frac{\partial\varphi}{\partial\theta} + \frac{1}{R^2}\frac{\partial^2\varphi}{\partial\theta^2} - \exp(\psi)\varphi = -[n - \exp(\psi) + \psi\exp(\psi)]. \tag{8}$$

Equations (1)–(3) and (8) are solved by the finite-difference method. Initial conditions are $n = 1$ and u=0 everywhere. Boundary conditions are $\varphi = \varphi(\tau)$ on the target and in φ=0 the plasma, and $\partial\varphi/\partial\theta = 0$ on the symmetry axis.

The normalized potential φ, ion density n and the ion velocity u in the simulation region are obtained by using the finite-difference method. Thus, the ion flux Γ to the surface of the vessel can be determined by

$$\Gamma = nu_{\perp}, \tag{9}$$

where $u_{\perp}$ is the normal ion velocity to the target surface. The power of the ion heating can be obtained through the normalized ion flux Γ.

When ions impact it, the target surface is directly heated by the incident ion-flux during the PSII, and the energy deposited by the ions is used as an input parameter. In general, the temperature distribution within the target is governed by a time-dependent partial differential equation with nonlinear boundary conditions due to radiative cooling.[13] The equation can be written as

$$\rho c\frac{\partial T}{\partial t} + H = \nabla \cdot k\nabla T, \tag{10}$$

where ρ is the density of the target material, c is the heat capacity, k is the thermal conductivity, and H is the resultant power of heating and cooling due to ion bombardment and thermal radiation respectively. If the thermal conductivity is uniform throughout the target and independent of temperature, this equation becomes

$$\rho c\frac{\partial T}{\partial t} + H = k\nabla^2 T. \tag{11}$$

The target temperature can be calculated by solving a two-dimensional unsteady-state heat transfer equation using finite difference. In spherical coordinates, the equation is

$$k\left[\frac{1}{r^2}\frac{\partial}{\partial r}\left(r^2\frac{\partial T}{\partial r}\right) + \frac{1}{r^2\sin\theta}\frac{\partial}{\partial\theta}\left(\sin\theta\frac{\partial T}{\partial\theta}\right)\right] + H = \rho c\frac{\partial T}{\partial t}. \tag{12}$$

In our model, the energy deposited by implanted ions, derived from the above sheath dynamics simulation, is used as a heat input and we ignore the volumetric effects. Meanwhile, we divide the full cycle of pulse into 14 time-intervals. Since temperature rise contributed by a single pulse is relatively small,[10] the target temperature can be modelled by averaging the input power over each time interval. The radiation from the target surface to the chamber wall is primary heat loss mechanism. We assume that the chamber wall temperature is water-cooled down to 22°C and the initial temperature of the target is taken as 22°C.

The radiative cooling can be modelled with the following equation:

$$P_{\mathrm{r}} = F\varepsilon\sigma(T^4 - T_{\mathrm{b}}^4), \tag{13}$$

where P_{r} is the net heat flux lost due to radiation to the chamber, F is the radiative shape factor for radiation from the target to the chamber, ε is the emissivity of the radiating surface, σ is the Stefan–Boltzmann constant, and T_{b} is the chamber temperature.

Because the hemispherical bowl is enclosed in the chamber and all the radiation leaving the target surfaces reaches the chamber wall, the shape factor F depends on the geometrical shape and arrangement of the surfaces of the bowl with respect to the chamber wall. The shape factor for an area element $\mathrm{d}A_1$ on the target is given by[14]

$$F = \int_{A_2} \frac{\cos\theta_1\cos\theta_2}{\pi S^2}\mathrm{d}A_2, \tag{14}$$

where the integration limits on the chamber wall area A_2 extend over only the portion that can be viewed by an area element $\mathrm{d}A_1$ on the target surface. The elements $\mathrm{d}A_1$ and $\mathrm{d}A_2$ have their normals at angles θ_1 and θ_2 to the line of length S joining them. For the outer surface and the brim surface of the bowl the integration calculated over a hemispherical surface centered at $\mathrm{d}A_1$, is 1.0. For the inner surface the integration calculated over the circular disk of the bowl opening, is 0.5. The method of calculation is shown in the Appendix.

3. Results and discussion

In our simulation, the hemispherical bowl with an inner radius r_{in}=40mm and an outer r_{out}=44mm is located in the plasma. The plasma has N_2^+ with a density of $6.8 \times 10^9 cm^{-3}$ and an electron temperature of 1.5eV. The applied potential is initially zero and rises (in the negative polarity) at a rate of 120kV/μs until it reaches a plateau value of –20kV and maintains this value. These simulation parameters are chosen based on the real experimental parameters.

The spatial distribution of the normalized ion flux along the surfaces of the vessel from inner bottom centre to the outer's for each pulse is shown in Fig.2. The ion flux on the target is very uneven. There are three peaks near the brim of the vessel where the electric field is concentrated: the middle one is at the centre of the brim, the left one is at the inner surface near the brim, and the other is at the outer surface.

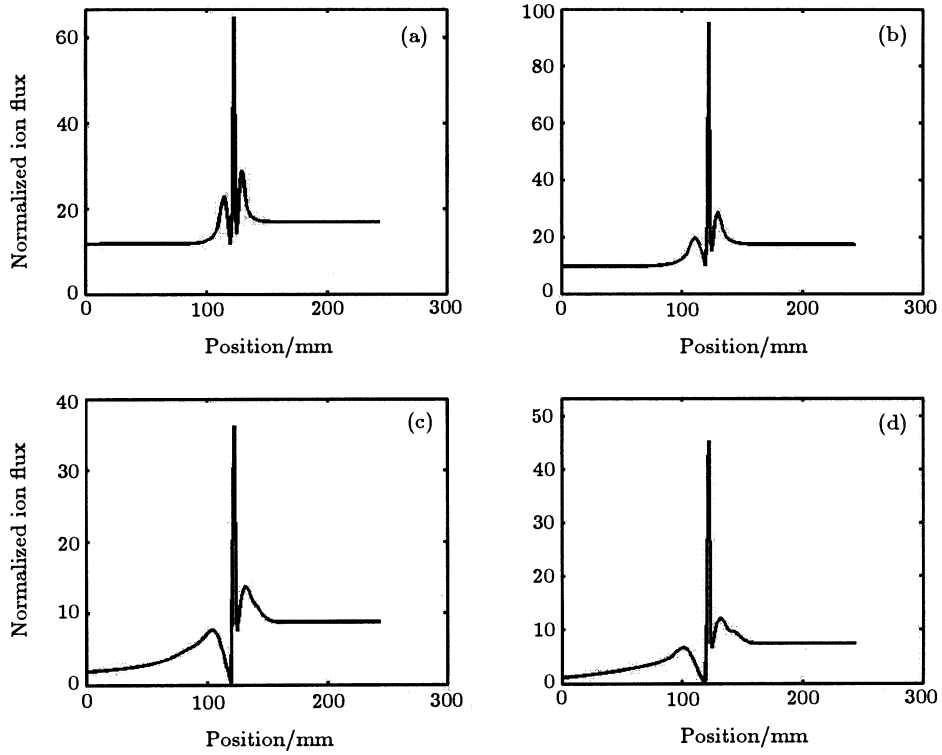


Fig.2. Normalized ion flux on the surface from the inner bottom centre to the outer's for normalized time (a) τ=1.0, (b) τ=3.0, (c) τ=15.0 and (d) τ=18.0.

In the temperature simulation, the density of the bowl material ρ is 8020kg/m^3 for stainless steel, c is 460J/(kg·K), and k is 30W/mK. The temperature distribution along the surface (arc direction) and the thickness (radial direction) of the bowl obtained for an implantation voltage with a pulsing frequency of 300Hz and a pulse duration of 16μs is depicted in Fig.3. The target temperature near the brim of the bowl is always higher than near the bottom, and it can be attributed to the higher heating flux. The target temperature rises rapidly initially but more slowly later due to the higher radiation heat loss at higher temperatures. At some time, the temperature distribution inside the bowl material reaches a steady state in which the temperature does not change. The target temperature attains equilibrium after 2400 seconds, as shown in Fig.4.

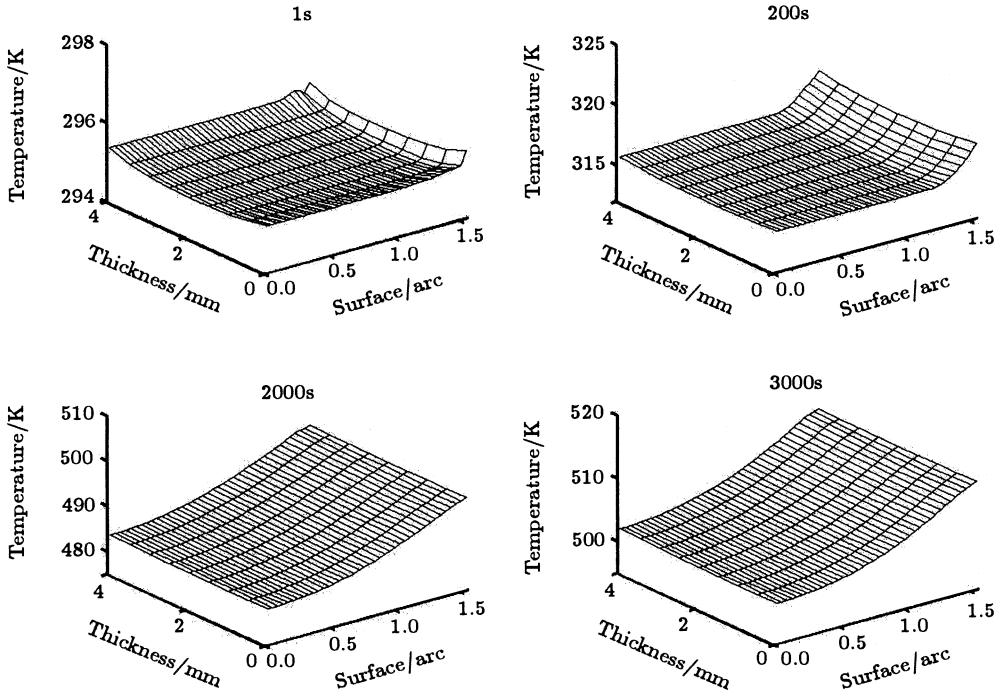


Fig.3. Two-dimensional temperature distribution on the bowl respectively at 1s, 200s, 4000s, and 6000s.

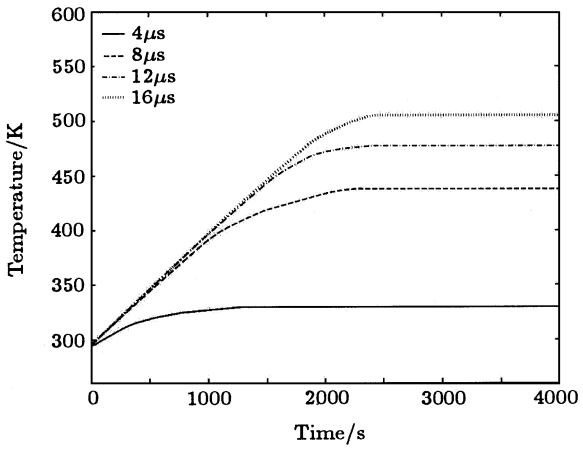


Fig.4. Effect of the pulse duration on the average temperature of the bowl.

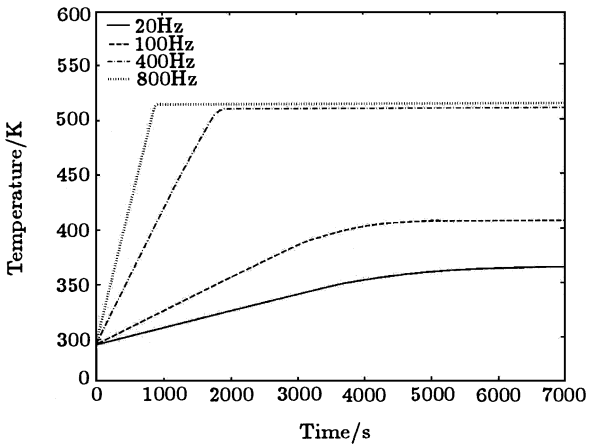


Fig.5. Effect of the pulsing frequency on the average temperature of the bowl.

Figure 4 shows the influence of the pulse duration on the average temperature of the bowl. The comparison indicates that equilibrium time within which the bowl temperature attains equilibrium increases with the increase of the pulse duration below some value of the pulse duration. If the pulse duration is over some value, the steady-state temperature of the bowl increases with the increase of the pulse duration while the equilibrium time will no longer increase. For a pulse of 300Hz/4μs, the bowl temperature reaches near-equilibrium after 1300 seconds. When the pulse duration increases to 16μs, the equilibrium time increases up to 2480 seconds. Meanwhile, the steady-state temperature increases from 329 to 505K.

The time dependence of the average temperature of the bowl for different frequencies is plotted in Fig.5 for a pulse duration of 16μs. It is seen that the equilibrium time decreases with the increase of pulsing frequency while the steady-state temperature of the bowl increases with the increase of pulsing frequency. If the pulsing frequency is over some value, the steady-state temperature of the bowl no longer increases. Our results indicate that the pulse duration over some value has no effect on the equilibrium time, and the pulsing frequency over some value has no effect on the steady-state temperature of the bowl either.

4. Conclusions

A model has been developed for predicting the 2D time-dependent temperature distribution of a hemispherical bowl-shaped vessel in plasma source ion implantation. The 2D fluid model and 2D temperature governing equation are used to describe the temperature rise and variation on the bowl. The different shape factors of the bowl for radiation from the inner and outer surfaces are taken into account in radiative energy loss. The results show that the temperature near the brim of the bowl is always higher than near the bottom, and a steady state in which the temperature distribution does not change can be reached after some time. The results also indicate that the time within which the bowl temperature attains equilibrium decreases with the increase of pulse duration while the temperature of the bowl in the steady state increases. It is noted that the equilibrium time and the steady-state temperature of the bowl will no longer have any change with the increase of the pulsing frequency over some value. Therefore, in the case where high temperature is desired, it is not effective to apply a voltage with a higher pulsing frequency.

Appendix: shape factor between a differential element on the inner surface of the hemispherical target and the chamber wall

Consider a spherical surface with a radius R as shown in Fig.6. The right half of it is assumed to be the inner surface of the hemispherical bowl-shaped target (solid case). Since the energy radiated from an elemental area on the inner surface of the hemispherical target to the chamber wall transfers through the opening of the bowl, Eq.(14) can be integrated over the other hemispherical surface with the same radius R (dashed case).

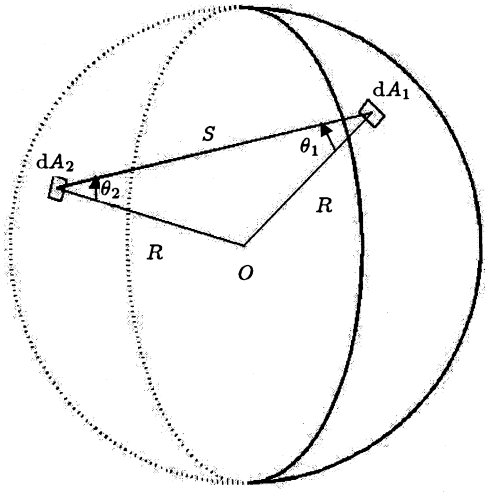


Fig.6. Geometry involved in the radiation within the hemispherical bowl-shaped vessel.

Since the sphere radius is normal to both element $\mathrm{d}A_1$ and $\mathrm{d}A_2$, the distance between these elements is given by $S = 2R\cos\theta_1 = 2R\cos\theta_2$ then Eq.(14) becomes

$$F = \frac{1}{4\pi R^2}\int_{A_2} \mathrm{d}A_2 = \frac{1}{2}.$$

References

[1] Conrad J R, Radtke J L, Doodd R A, Worzala F J and Tran N C 1987 *J. Appl. Phys.* **62** 4591

[2] Walter K C, Scheuer J T, McIntyre P C, Kodali P, Yu N and Nastasi M 1996 *Surf. Coat. Technol.* **85** 1

[3] Wang S Y, Chu P K, Tang B Y, Zeng X C and Wang X F 1997 *Nucl. Instrum. Methods. Phys.* **127/128** 1000

[4] Walter K C, Dodd R A and Conrad J R 1995 *Nucl. Instrum. Methods Phys. Res.* B **106** 522

[5] Chu P K, Qin S, Chan C, Cheung N W and Larson L A 1996 *Mater. Sci. Eng. R.* **17** 207

[6] Walter K C, Nastasi M and Munson C 1997 *Surf. Coat. Technol.* **93** 287

[7] Scheridan T E and Alport M J 1994 *Appl. Phys. Lett.* **64** 1738

[8] Scheridan T E 1995 *J. Phys.* D: *Appl. Phys.* **28** 1094

[9] Scheridan T E, Kwok T K and Chu P K 1998 *Appl. Phys. Lett.* **72** 1829

[10] Tian X B and Chu P K 2001 *J. Phys.* D: *Appl. Phys.* **34** 1639

[11] Liu C S and Wang D Z 2003 *Surf. Coat. Technol.* **171** 119

[12] Blanchard J P 1994 *J. Vac. Sci. Technol.* B **12** 910

[13] Siegel Robert and Howell J R 1981 *Thermal Radiation Heat Transfer* (New York: Hemisphere) p271